

# Optical system of the Three Antarctic Survey Telescopes

Xiangyan Yuan<sup>1,2,3★</sup> and Ding-qiang Su<sup>4,5,1</sup>

<sup>1</sup>National Astronomical Observatories/Nanjing Institute of Astronomical Optics and Technology, Chinese Academy of Sciences, 188 Bancang Street, Nanjing 210042, China

<sup>2</sup>Key Laboratory of Astronomical Optics and Technology, Nanjing Institute of Astronomical Optics and Technology, Chinese Academy of Sciences, China

<sup>3</sup>Chinese Center for Antarctic Astronomy, China

<sup>4</sup>Department of Astronomy, Nanjing University, 22 Hankou Road, Nanjing 210093, China

<sup>5</sup>Key Laboratory of Modern Astronomy and Astrophysics (Nanjing University), Ministry of Education, China

Accepted 2012 March 5. Received 2012 March 4; in original form 2011 December 22

## ABSTRACT

Dome A is the highest point on the Antarctic Plateau, and the Chinese Expedition Team first arrived here in 2005 January. It is an excellent site for astronomical observations. The first-generation Chinese Antarctic optical telescope CSTAR has been operating on Dome A since 2008 January. The second-generation Chinese telescopes known as the Three Antarctic Survey Telescopes (AST3) are currently being developed. AST3 includes three telescopes matched respectively with *G*-, *R*- and *I*-band filters. Each telescope is a catadioptric optical telescope with an entrance pupil diameter of 500 mm, an *f*-ratio of 3.73 and a field of view of 4°14′. The optical system of the AST3 consists of a transparent aspherical plate, an aspherical primary mirror and a spherical refractive corrector with a filter before the focal plane. The main features of the AST3 are the following: good image quality, a planar focal plane, reduced atmospheric dispersion, an absence of distortion and a compact structure. The main scientific goal of the AST3 is to survey the sky. In 2012 January, the first telescope of the AST3 was successfully installed on Dome A.

**Key words:** atmospheric effects – techniques: miscellaneous – telescopes – surveys – stars: imaging.

## 1 INTRODUCTION

Lawrence et al. (2004) have shown that Dome C on the Antarctic Plateau is the best site on Earth for astronomical observations. It has a mean seeing of 0.27 arcsec above 30 m from the ground. Dome A has a latitude 80°22′02″S, a longitude 77°32′21″E and an elevation of 4093 m, and it is the highest point on the Antarctic Plateau (Hou et al. 2007). It was first visited by the Chinese Expedition Team in 2005 January. Preliminary site testing, led by the Chinese Center of Antarctic Astronomy (CCAA), has shown that Dome A can be reasonably predicted to be an excellent site for astronomical observations – it could be as good as Dome C, or even better (Bonner et al. 2010; Yang et al. 2010). China is actively promoting astronomical observations in the Antarctic. The first-generation Chinese Antarctic optical telescope is known as the Chinese Small Telescope Array (CSTAR; Liu & Yuan 2009). It was composed of four identical telescopes, with a 145-mm entrance pupil, a 20-deg<sup>2</sup> field of view (FOV) and four different filters (*G*, *R*, *I* and open band). CSTAR was mainly used for the detection of variable sources, and for the measurement of atmosphere extinction, sky brightness and cloud coverage (Zou et al. 2010). CSTAR was deployed on Antarctic

Dome A in 2008 January and its automatic operation continued for four consecutive winters. The Three Antarctic Survey Telescopes (AST3; see Fig. 1) are the second-generation Chinese telescopes on Dome A. Each of the telescopes of the AST3 has a 500-mm entrance pupil diameter, an *f*-ratio of 3.73 and a FOV of 4°14′ (2°92′ × 2°92′), and each is matched with one of the three different (*G*, *R* and *I*) filters (Yuan et al. 2010). For the AST3, the main sky area for observations is a zenith distance less than 70°. The optical system of the AST3 consists of a transparent aspherical plate, an oblate primary mirror with a diameter of 680 mm and a spherical refractive corrector with a filter before the focal plane. The main features of the AST3 are the following: good image quality, a planar focal surface, reduced atmospheric dispersion and an absence of distortion. The optical length and the diameter of the primary mirror are significantly smaller than a typical Schmidt system. Because of the excellent conditions at Dome A, such as the high atmospheric transparency, very good seeing, lowest water vapour, lower wind speed and boundary layer, and because there are more than three months of continuous observation time per year, many scientific projects can be carried out by the AST3. These include a survey of Type Ia supernovae to study the dark energy of the Universe (Kim et al. 2010) and microlensing to search for exoplanets and to find new variable sources, etc. The detailed scientific goals of the AST3, which have mainly been conceived by Professor Lifan Wang, will

★E-mail: xyuyan@niaot.ac.cn



**Figure 1.** The first telescope of the AST3, without dome (left) and covered by dome (right).

soon be published in a separate paper. The AST3 can also be used for site testing, including the measurements of seeing, atmosphere extinction and sky brightness. The first telescope of the AST3 for the *I* band has been completed, and it was installed on Dome A in 2012 January. The other two telescopes of the AST3 will be installed there at a later date. Then, the three telescopes with their respective *G*, *R* and *I* filters will perform simultaneous observations on Dome A. The third-generation Chinese Antarctic telescopes are being designed, and these include a 2.5-m optical/infrared telescope and a 5-m submillimetre telescope.

## 2 FORMATION OF THE CONFIGURATION OF THE OPTICAL SYSTEM OF AST3

The Schmidt telescope (Schmidt system) was invented by B. V. Schmidt in 1931. Its key feature is the placement of a transparent aspherical plate at the curvature centre of a spherical mirror (Fig. 2a). Because of the system's symmetry for on-axis and off-axis light, such an optical system can deliver very good and distortion-free images over a large FOV. The shortcomings of the Schmidt telescope include the long tube, the large spherical primary mirror and the curved focal surface. Su (1962) studied the Schmidt telescope further and pointed out that if the aspherical plate was put at the focus of the primary mirror and the primary mirror was changed into a proper aspherical shape (Fig. 2b), then both the spherical aberration and coma could be eliminated. In such a system, the length of the tube can be half the original length of the Schmidt system, and the difference in diameter between the primary mirror and the aspherical plate is halved. However, there is astigmatism in this system. In 1980, Lanjuan Wang and Ding-qiang Su thought of adding another transparent aspherical plate before the focus, which could make the system free of spherical aberration, coma and astigmatism (Fig. 2c). Because the symmetry of this system is not as good as that of the Schmidt telescope, the off-axis image spot is larger than that of the Schmidt telescope and there is distortion. After this research was completed, Wang and Su found that Brown (1970) had already proposed this type of system (Fig. 2c). In 1981, the work of Wang and Su was presented as a paper at the ICO-12

Conference (Graz/Austria). A version of this paper, abridged and inappropriately modified by the editor, can be found in *Acta Optica Sinica* (Wang & Su 1983).

For Antarctic telescopes, although image quality is essential, a compact configuration is also important for their transportation, installation and operation. Besides the planar focal surface, the correction of atmospheric dispersion and the absence of distortion are also crucial. Since the 1980s, some atmospheric dispersion correctors for larger FOV telescopes have been designed (e.g. Epps, Angle & Anderson 1984; Su 1986; Su & Liang 1986; Wynne 1986, 1988; Wang & Su 1990; Su, Jia & Liu 2012). In these correctors, there is a pair of prisms or lens-prisms. Each of these is a cemented lens, with a tilted cemented surface, and each consists of two different glasses. As these two lens-prisms are rotated, different dispersions can be obtained. Among these designs, Su (1986) was the first to propose the use of two lens-prisms to correct both the atmospheric dispersion and the telescope aberrations. At the initial stage in the design of the AST3, the classical Schmidt system, the Schmidt-Cassegrain system and the short-tube catadioptric system mentioned above were considered. After computation and comparison, the short-tube catadioptric system (Fig. 2c) was adopted. In the design, Yuan introduced the important improvement – a refractive corrector, which contains only spherical surfaces and includes a lens-prism, is used to replace the transparent aspherical plate before the focus (Fig. 2d). Thus, in the AST3, the focal surface is planar, atmospheric dispersion is reduced and distortion is eliminated.

The abbreviation AST3 was once meant to stand for Three Antarctic Schmidt Telescopes (Yuan et al. 2010). However, because the key features of the Schmidt telescope no longer exist in the telescopes under design, we have changed the name to the Three Antarctic Survey Telescopes, still designated by the same abbreviation (AST3).

## 3 DESIGN OF THE OPTICAL SYSTEM

The optical system of the AST3 consists of a transparent aspheric plate, an oblate primary mirror and a spherical lens corrector including a filter before the focal plane. The ZEMAX software was

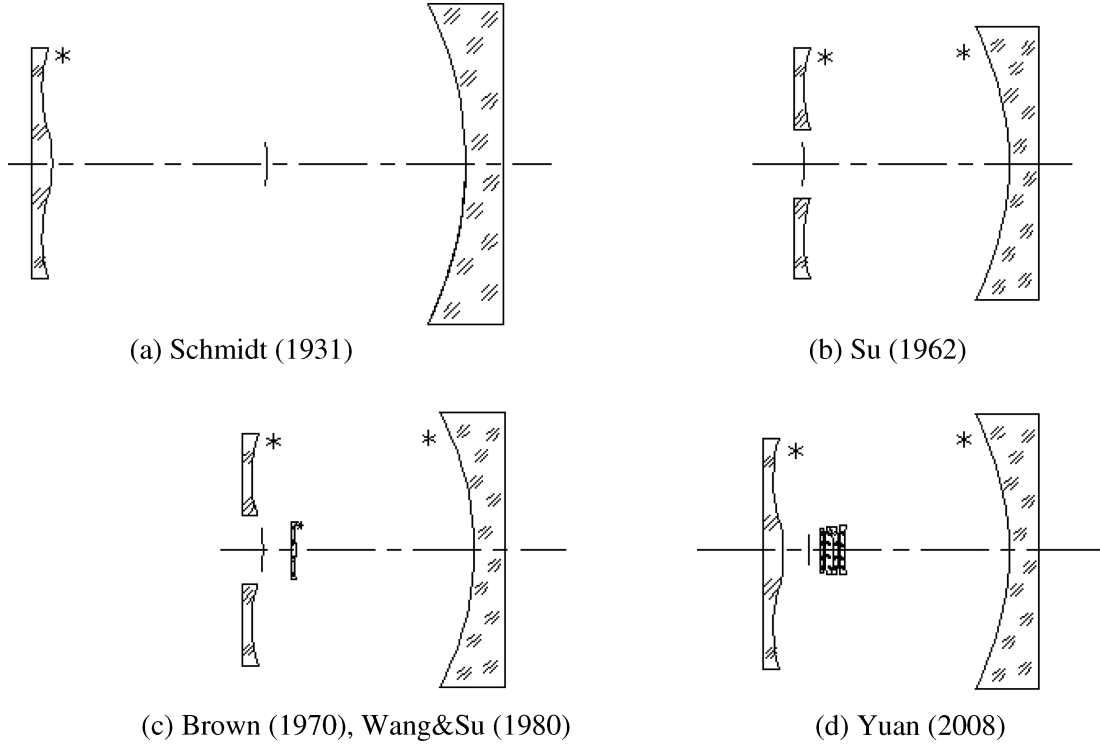


Figure 2. The evolution of the optical system from Schmidt to AST3 (\* means aspherical surface).

used for the optimization of this system. In order to reduce complexity and to increase reliability during the corrector design, Yuan did not use a pair of rotating lens–prisms to compensate for different dispersions; only one lens–prism is included. Because the cemented surface is not safe enough at very low temperatures, the two single lenses of the lens–prism were set apart at a slight distance of 0.1 mm. First, in the optimization of the optical system, the atmospheric dispersion was not considered (i.e. all optical surfaces were coaxial including the middle surfaces of the lens–prism). Next, without changing any other parameters, Yuan tilted only the middle surfaces of the lens–prism in order to make this optical system produce a 1.17-arcsec dispersion for the *G* band, which corresponds to atmospheric dispersion at  $z = 56^\circ$ . The optical system is shown in Figs 3 and 4. The optical parameters of the AST3 are listed in Table 1.

A  $10 \times 10$  K CCD from STA, with pixel size of  $9 \mu\text{m}$ , is used for the AST3 detector. Although the off-axis image spot of the AST3 is larger than that of the Schmidt telescope, it meets the requirement of 80 per cent light energy within 1 arcsec, and it is a good match for the CCD pixel size. Many other features of the AST3 are superior to those of the Schmidt telescope.

According to the science requirements and the selected CCD, the main specifications of the designed optical system are the following.

- (i) The entrance pupil diameter is 500 mm.
- (ii) The primary mirror diameter is 680 mm.
- (iii) The focal length is 1867 mm.
- (iv) The  $f$ -ratio is 3.73.
- (v) The FOV is  $4^\circ 14'$ .
- (vi) The working wavelength is 400–900 nm, with a *G* (400–550 nm), *R* (560–700 nm) and *I* (685–840 nm) filter, respectively, for each of the telescopes of the AST3.

(vii) The image quality is 80 per cent light energy encircled in 1 arcsec, not considering dispersion (the image spot of the *I* band is shown in Fig. 5).

(viii) The largest distortion in the whole FOV is 0.012 per cent (less than one pixel of the CCD).

(ix) The total optical length is 2.4 m.

(x) The shape of the inner surface of the aspherical plate can be expressed as

$$z = \frac{cr^2}{1 + \sqrt{1 - (1+k)c^2r^2}} + \alpha_1 r^2 + \alpha_2 r^4 + \alpha_3 r^6 + \alpha_4 r^8, \quad (1)$$

where  $c = 0$ ,  $\alpha_1 = -8.4659 \times 10^{-6}$ ,  $\alpha_2 = 1.5716 \times 10^{-11}$ ,  $\alpha_3 = 2.501 \times 10^{-18}$ ,  $\alpha_4 = -5.753 \times 10^{-24}$ , and the units of  $r$  are millimetres.

## 4 CHARACTER OF THE OPTICAL SYSTEM OF THE AST3

### 4.1 General features of the optical system of the AST3

Each of the telescopes of the AST3 is characterized by good image quality, a planar focal surface, reduced atmospheric dispersion and eliminated distortion. In any wavelength band of *R* and *I*, 80 per cent of the light energy of each image spot at  $50^\circ \leq z \leq 70^\circ$  is within 1 arcsec (about one pixel of the CCD). In the sky area  $z \leq 70^\circ$  of observations, the maximum of celestial object dispersion is reduced from 2.49 to 1.4 arcsec with the *G* band (the atmospheric dispersion reaches its maximum in this band). The largest distortion is 0.012 per cent (less than one pixel of the CCD) in the whole FOV. The structure of the AST3 is compact.

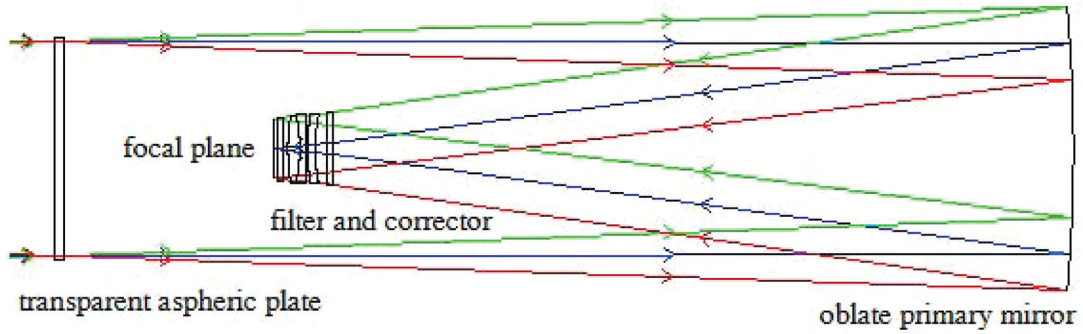


**Figure 3.** The optical layout of the AST3.

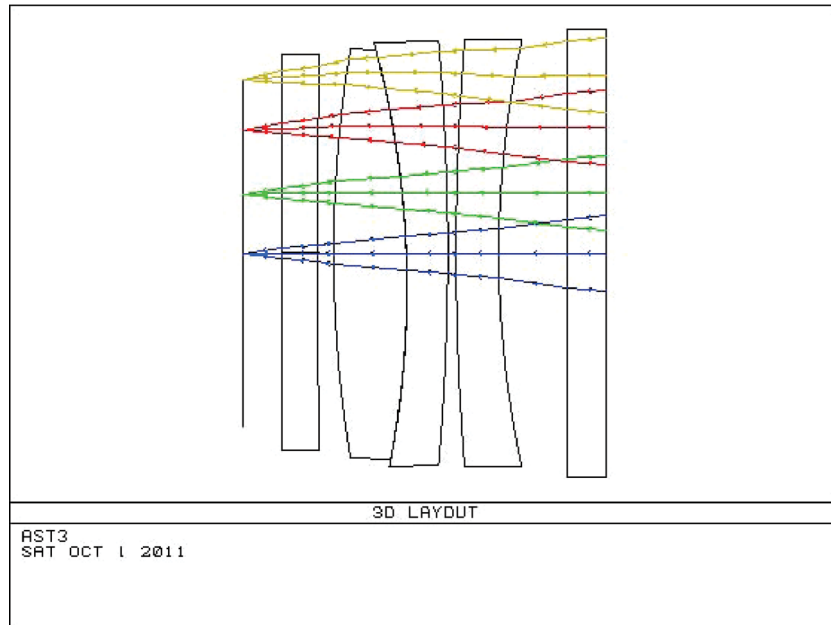


**Figure 4.** The optical layout of the AST3 corrector before the focal plane. (Along the optical path, the lenses are the filter, lens 1, lens–prism and lens 2, which is also used as the CCD sealing window. The last surface shows the CCD.)

**Table 1.** The optical parameters of the AST3.

Optical element	Radii (mm)	Conic coefficient	Thickness (mm)	Diameter (mm)	Glass
Aspherical plate	Infinity	0	25	502	Fused silica
	Aspherical	0	2370	500	
Primary mirror	−3752	0.677	1739.65	666	Zerodur
Filter	Infinity	0	15.5	173	Fused silica
	Infinity	0	26.182		
Lens 1	385.71	0	16.5	165	Fused silica
	1013.9	0	3.21		
Part A of lens–prism	−934.21	0	16	164	LLF1
	−358(tilted 2.1°)	0	0.1		
Part B of lens–prism	−358(tilted 2.1°)	0	28	158	N-PSK3
	482.1	0	6.37		
Lens 2	3204.89	0	13.5	153.28	Fused silica
	Infinity	0	15		
Focal plane	Infinity			134.6	

#### 4.2 Image spot size

When either atmospheric dispersion or lens–prism dispersion exists, or if both exist, the images are not rotationally symmetric in the

whole FOV. Table 2 gives the maximum image spot diameter with 80 per cent encircled energy, through the atmosphere and the AST3, in the whole FOV. For comparison, the image quality of the lens–prism without a tilted surface is also listed.

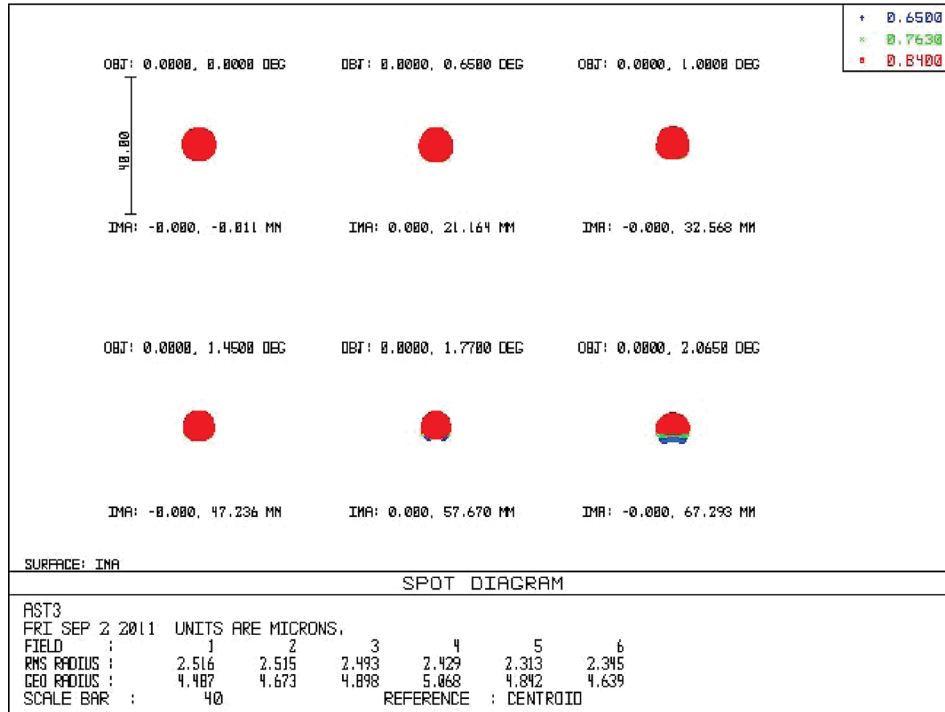


Figure 5. The *I*-band image spot diagram through the atmosphere and AST3 (on the scale bar, 40  $\mu\text{m}$  corresponds to 4.4 arcsec).

**Table 2.** The maximum image spot diameter with 80 percent encircled energy, through the atmosphere and AST3, in the whole FOV (the units are  $\mu\text{m}$ ; 10  $\mu\text{m}$  corresponds to 1.1 arcsec).

		Filter <i>G</i> (400–550 nm)	Filter <i>R</i> (560–700 nm)	Filter <i>I</i> (685–840 nm)
$z = 50^\circ$	Case A <sup>a</sup>	11.2	5.2	7.4
	Case B <sup>b</sup>	7.7	4.2	7.3
$z = 56^\circ$	Case A	13.2	6.8	7.4
	Case B	7.6	4.5	7.3
$z = 70^\circ$	Case A	22.4	9.2	8.6
	Case B	12.6	6.3	7.6

<sup>a</sup>Case A corresponds to the lens–prism without a tilted surface.

<sup>b</sup>Case B corresponds to the lens–prism with a tilted surface.

### 4.3 Dispersion of celestial object

Among the *G*, *R* and *I* bands, the largest atmospheric dispersion occurs in the *G* band and the minimum occurs in the *I* band. The average winter temperature at Dome A is about  $-65^\circ\text{C}$  to  $-70^\circ\text{C}$ . We suppose it to be  $-70^\circ\text{C}$ , with an elevation of 4093 m and with atmospheric pressure of 0.57. The atmospheric dispersions under zenith distances  $50^\circ$  and  $70^\circ$  are 1 and 2.2 arcsec, respectively, for the *G* band. Only one lens–prism is used in the AST3. The dispersion of the AST3 for the *G* band is 1.17 arcsec, which corresponds to atmospheric dispersion at  $z = 56^\circ$ . So, the dispersion of the celestial object at  $z = 56^\circ$  is compensated; at  $z = 70^\circ$ , it is reduced from 2.2 to 1.03 arcsec; at the zenith, it changes to 1.17 arcsec from zero; at  $z = 40^\circ$ , it is half of 1.17 arcsec. The ratio of the sky area of  $z \leq 40^\circ$  to  $z \leq 70^\circ$  is 0.36. By using a lens–prism in the AST3, the concise conclusions about the dispersion of the celestial object are the following: (i) improvement for 64 percent of the sky area and deterioration for 36 percent of the sky area; (ii) reduction of the maximum dispersion from 2.2 to 1.17 arcsec for the *G* band.

The AST3 are equatorial mounting telescopes. The dispersion of the lens–prism is always along the declination direction (the direction of the celestial pole), not the zenith direction. So, the above results are approximate. However, because the latitude of Dome A is  $80^\circ 22'$ , the error for the above results is very small.

### 4.4 Two examples

#### 4.4.1 Example 1 for the *I* band

Because both the atmospheric dispersion and dispersion of the lens–prism are small in this band, the difference in image quality between the tilted and non-tilted surfaces of the lens–prism is small, and the images in the whole FOV are nearly rotationally symmetric. So, here, only a spot diagram (Fig. 5) through the atmosphere and the AST3 is given, with  $z = 50^\circ$ , the lens–prism dispersion and all image spots along the zenith direction.

#### 4.4.2 Example 2 for the *G* band

If the middle surface of the lens–prism is not tilted, the maximum image spot of the *G* band will disperse up to about 1.12 and 2.49 arcsec at  $z = 50^\circ$  and  $70^\circ$ , respectively ( $z = 50^\circ$  and  $70^\circ$  correspond to the upper transit and lower transit positions of the celestial object with  $\delta = -30^\circ$ ). In the AST3, the middle surface of the lens–prism is tilted and the maximum image spot is greatly reduced. For the sake of brevity, here we only give two spot diagrams through the atmosphere and the AST3, with  $z = 50^\circ$ , with all image spots along the zenith direction and with the middle surface of the lens–prism not tilted (Fig. 6) and tilted (Fig. 7). From Table 2 and Figs 6 and 7, we can see that for the *G* band, when the middle surface of the lens–prism is tilted (as in the AST3), the image quality is clearly improved.



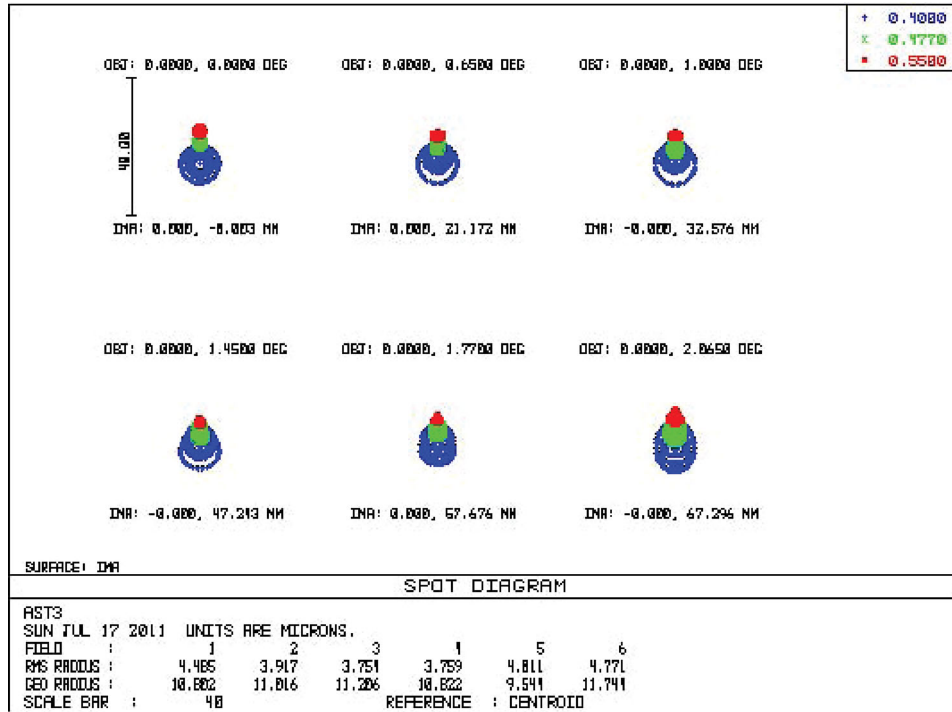


**Figure 6.** The G-band image spot with zenith distance  $50^\circ$  if the middle surfaces of the lens–prism are not tilted (i.e. atmospheric dispersion is not corrected). The scale bar is  $40\ \mu\text{m}$ .

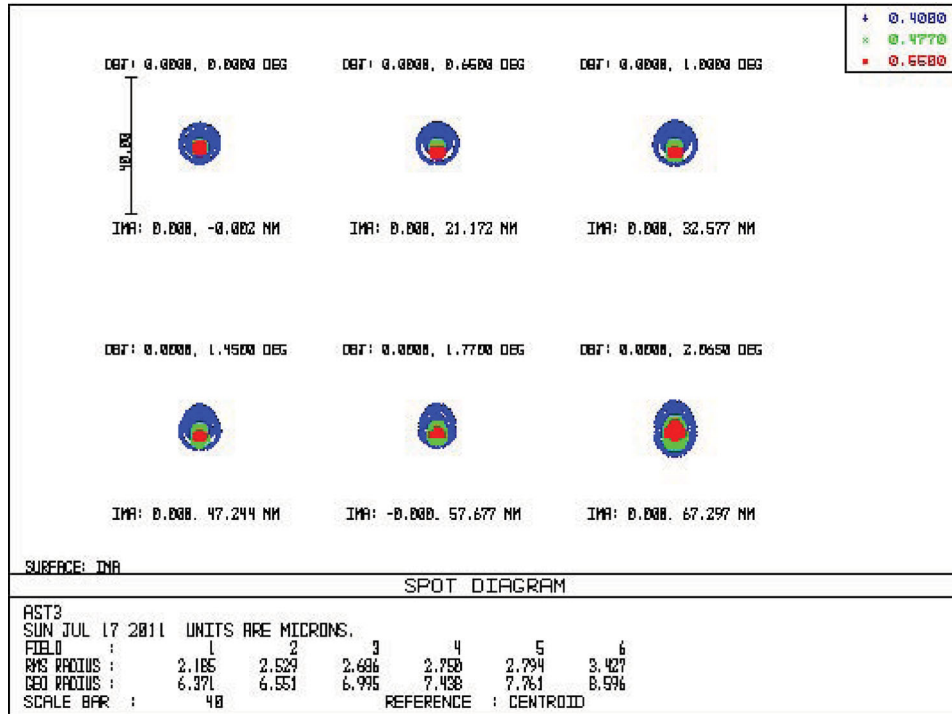


**Figure 7.** The G-band image spot with zenith distance  $50^\circ$  if the middle surfaces of the lens–prism are tilted (i.e. atmospheric dispersion is corrected, in the AST3). The scale bar is  $40\ \mu\text{m}$ .

#### 4.5 Results of test observations

From 2011 August 29 to October 16, we performed test observations of the first AST3 telescope with the *I* band filter at Xuyi Station of the Purple Mountain Observatory, Chinese Academy of Sciences,

in Jiangsu Province (latitude  $N32^\circ44'$ , longitude  $E118^\circ28'$ ). After fine alignment of the optical system, we pointed the telescope to the Double Cluster (NGC 884) with zenith distance about  $34^\circ$ . We obtained a very uniform image in a full FOV with an exposure time of 1 s. The seeing was about 2.2–2.7 arcsec during the observation

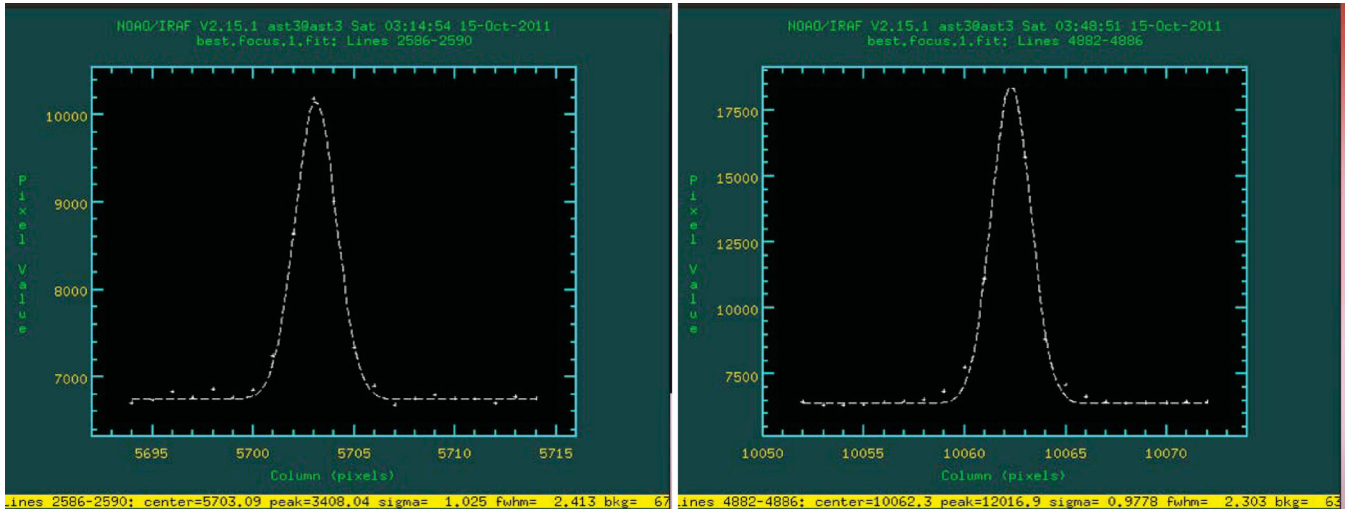


**Figure 8.** Two star profiles from the first telescope of the AST3 with the *I*-band filter at the centre and edge of the CCD with an exposure time of 1 s.

time measured by a DIMM. The profiles of two star-spots at the centre and top right of the image are shown in Fig. 8, and these show a very good fit to the Gaussian profile with FWHM of 2.4 and 2.3 arcsec, respectively.

#### 4.6 Possible improvement and a new idea

At present, we are considering that if the first telescope of the AST3 works very well on Dome A, a pair of lens–prisms might be adopted in the corrector design of the second telescope of the AST3. In this way, the atmospheric dispersion in the full observation area  $z \leq 70^\circ$  can be compensated for by the rotation of these two lens–prisms.

Thus, we can hopefully use a pair of lens–prisms to produce a dispersion of about 5–10 arcsec. Su suggests the application

of such an extra-low dispersion spectrum in lieu of multicolour photometry for celestial objects in the whole FOV. Because such work requires that the sky brightness should be as low as possible, space and Dome A are ideal sites. We are considering the possibility of such work for the third-generation Chinese Antarctic 2.5-m telescope, and even for the second telescope of the AST3.

## 5 OPTICAL THERMAL ANALYSIS

Because the telescope was developed under normal temperature and pressure, with the very low temperatures (as low as  $-83^\circ\text{C}$  in winter) on Dome A in the Antarctic, low-thermal-expansion materials need to be used for the main optical parts and for the structure in order

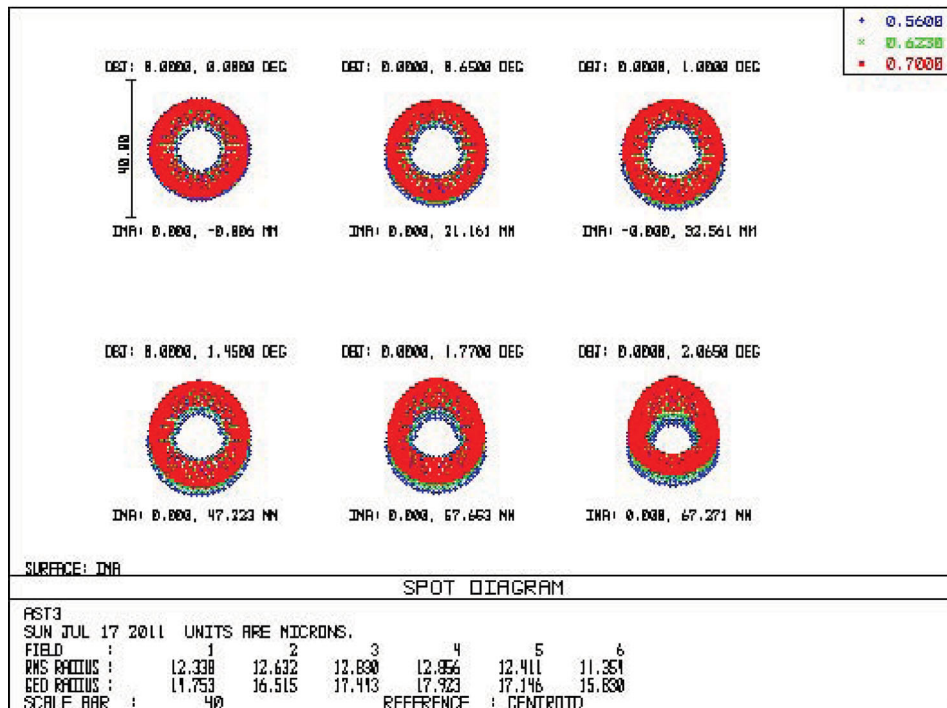


**Figure 9.** The simulated defocused *R*-band image spot during the winter at Dome A. The scale bar is 40  $\mu\text{m}$ .

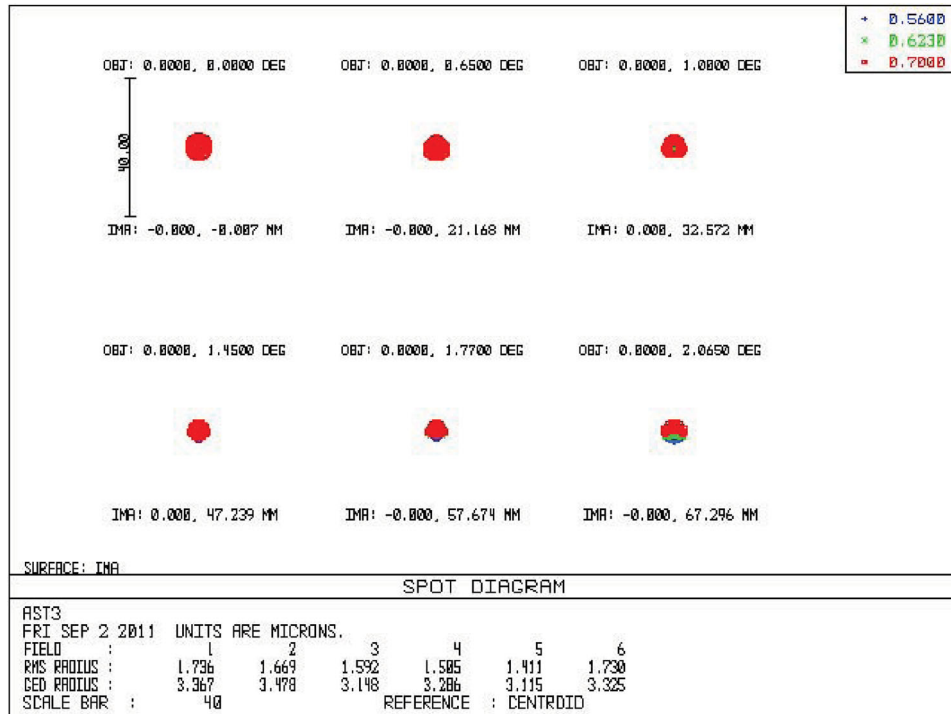


Figure 10. The *R*-band image spot after precise refocusing. The scale bar is 40  $\mu\text{m}$ .

to minimize the thermal effect and the shift of focus in the case of large temperature differences. Zerodur and fused silica were selected for most of the AST3's optical components except for the lens–prism of the corrector. INVAR36 was selected as the material for the main structure. A motorized focusing mechanism with a moving accuracy of 1  $\mu\text{m}$  was designed to adjust the focal plane to the best position in order to compensate for the thermal effect. This mechanism was successfully tested in a winterization chamber from a normal temperature down to  $-80^\circ\text{C}$ .

The thermal expansion coefficients of the Zerodur mirror, fused silica and INVAR36 were set to be  $0.1 \times 10^{-6}$ ,  $0.5 \times 10^{-6}$  and  $1.5 \times 10^{-6}$ , respectively, for the analysis. The telescopes of the AST3 are developed at a temperature of  $20^\circ\text{C}$ . At  $-40^\circ\text{C}$  and an atmospheric pressure of 0.57 (i.e. the conditions of late summer at Dome A), if we consider the thermal effect, the CCD box needs to move by 0.167 mm for focusing. Fig. 9 shows the *R*-band image spot of the AST3 at  $-80^\circ\text{C}$  and an atmospheric pressure of 0.57 at the focused position for the summer. Fig. 10 shows the refocused image spots after the CCD box has moved by 0.12 mm for refocusing. Of this 0.12 mm, only 0.014 mm is caused by the thermal effect of the optical components, and most of the rest is induced by the thermal effect of the structure.

## ACKNOWLEDGMENTS

We would like to thank Professors Xiangqun Cui, Yanan Wang, Yongtian Zhu, Lifan Wang and Genrong Liu for their useful discussions and suggestions for the design of the optical system of the AST3. We are grateful for the support of the Important Direction

Project of the Chinese Academy of Sciences (CAS) Knowledge Innovation Project (KJ CX2-EW-T04).

## REFERENCES

- Bonner C. S. et al., 2010, *PASP*, 122, 1122
- Brown D. S., 1970, in Dickson J. H., ed., *Proc. Optical Instruments and Techniques*. Oriel Press, Newcastle-upon-Tyne, p. 521
- Epps H. W., Angel J. R. P., Anderson E., 1984, in Ulrich M.-H., Kjar K., eds., *Proc. IAU Colloq. 79, Very Large Telescopes, Their Instrumentation and Programs*. ESO, Garching, p. 519
- Hou S., Li Y., Xiao C., Ren J., 2007, *Chin. Sci. Bull.*, 52, 428
- Kim A. et al., 2010, *Astropart. Phys.*, 33, 248
- Lawrence J. S., Ashley M. C. B., Tokovinin A., Travouillon T., 2004, *Nat*, 431, 278
- Liu G., Yuan X., 2009, *Acta Astron. Sinica*, 50, 224
- Su D., 1962, *J. Nanjing University (Astronomy)*, 25
- Su D., 1986, *A&A*, 156, 381
- Su D., Liang M., 1986, in Barr L. D., ed., *Proc. SPIE Conf. Ser. Vol. 628, Advanced Technology Optical Telescope III*. SPIE, Bellingham, p. 479
- Su D., Jia P., Liu G., 2012, *MNRAS*, 419, 3406
- Wang L., Su D., 1983, *Acta Opt. Sinica*, 3, 132
- Wang Y., Su D., 1990, *A&A*, 232, 589
- Wynne C. G., 1986, *Observatory*, 106, 163
- Wynne C. G., 1988, *MNRAS*, 230, 457
- Yang H. et al., 2010, *PASP*, 122, 490
- Yuan X. et al., 2010, in Stepp L. M., Gilmozzi R., Hall H. J., eds., *Proc. SPIE Conf. Ser. Vol. 7733, Ground-Based and Airborne Telescopes III*. SPIE, Bellingham, p. 77331V
- Zou H. et al., 2010, *AJ*, 140, 602

This paper has been typeset from a  $\text{\LaTeX}$  file prepared by the author.